Cooperative action of coherent groups in broadly heterogeneous populations of interacting chemical oscillators

A. S. Mikhailov*, D. H. Zanette*†, Y. M. Zhai‡, I. Z. Kiss‡, and J. L. Hudson‡§

*Abteilung Physikalische Chemie, Fritz-Haber-Institut der Max-Planck-Gesellschaft, Faradayweg 4-6, 14195 Berlin (Dahlem), Germany; †Centro Atómico Bariloche, 8400 San Carlos de Bariloche, Rio Negro, Argentina; and ‡Department of Chemical Engineering, 102 Engineers' Way, University of Virginia, Charlottesville, VA 22904

Communicated by Gerhard Ertl, Max Planck Institute for the Advancement of Science, Berlin, Germany, April 24, 2004 (received for review February 2, 2004)

We present laboratory experiments on the effects of global coupling in a population of electrochemical oscillators with a multimodal frequency distribution. The experiments show that complex collective signals are generated by this system through spontaneous emergence and joint operation of coherently acting groups representing hierarchically organized resonant clusters. Numerical simulations support these experimental findings. Our results suggest that some forms of internal self-organization, characteristic for complex multiagent systems, are already possible in simple chemical systems.

Currently, much interest is focused on the investigation of multiagent systems that are formed by a large number of interacting active elements. Such systems show a special kind of self-organization, characterized by spontaneous synchronization, dynamical clustering, and development of hierarchical order (1, 2). Individual agents may represent humans, animals, or robots and other artificially produced active units (3, 4). Depending on the nature of the elements, their mutual interactions, and the degree of synchronization, different collective tasks out of the reach of the individual agents can be exercised by their organized populations. The typical examples of multiagent systems belong to social sciences, but a question can be asked whether similar kinds of complex internal organization can emerge, in a primitive form, already in relatively simple chemical systems and may be employed for the purposes of chemical engineering. Experiments and numerical simulations reported in this article give evidence of complex cooperative action in populations of interacting electrochemical oscillators.

The importance of coherent dynamics resulting from synchronization in biological systems was noted by Wiener (5) and Winfree (6); synchronization plays a significant role in the operation of the brain (7) and in coherent flashing (8) and chirping (9) in large populations of fireflies or crickets. General theories describing the onset of synchronization for periodic and chaotic oscillators have been constructed (10–12) and confirmed in experiments (13). It has been shown that strong interaction among highly nonlinear identical dynamical elements produces clustering (11, 14–17). Less attention has, however, been paid to the analysis of spontaneous dynamical clustering in weakly interacting and broadly heterogeneous populations.

We address the problem of heterogeneous populations by using a model laboratory system, an array of electrochemical oscillators whose elements have a broad distribution of natural oscillation frequencies. The reported experiments, complemented by numerical simulations, exhibit characteristics typical of multiagent systems, including the emergence of complex collective signals through the cooperative action of coherent groups.

We present numerical simulations for a system of phase oscillators. A phase oscillator is a simple cyclic element (a clock) specified only by its natural frequency. We choose a population of 1,000 such oscillators with a strongly nonuniform distribution of natural frequencies displaying several maxima (Fig. 1*A*). When interactions among the elements were included, formation of synchronous oscillator groups was observed. Synchronization could clearly be seen by examining effective oscillation frequencies, defined as the average number of actual cycles per unit time for a given element. The distribution of effective frequencies at various interaction strengths is shown in Fig. 1*B*. As the interaction strength grew, small coherent oscillator groups with identical oscillation frequencies, different from their natural frequencies, appeared on the bulk background of nonentrained elements. For higher interaction strengths, most of the population was entrained into several large clusters. Eventually, the dynamics of the entire system became fully synchronized. Clustered states were observed in an interval of transition between complete incoherence and rigid full synchronization. It is inside this transition interval that the properties resembling social organization were found. The synchronization tree in Fig. 1*B* reveals the hierarchical organization of the population.

The ability to exercise collective tasks can be viewed as the essential property of any highly organized multiagent system. The oscillator population can indeed generate collective signals. As an example, we considered a complex-valued collective signal $z(t) = N^{-1}\sum_{j=1}^{N} \exp[i\phi_j(t)]$, where i is the imaginary unit, ϕ_j is the phase of the jth oscillator, and N is their total number. In the incoherent regime in the absence of interactions, the phases of individual elements were random and the collective signal almost vanished. Fig. 1*C* shows how the magnitude of z grew with the interaction strength, revealing gradual emergence of cooperative action through cluster formation. Fig. 1*D* shows the trajectories of $z(t)$ for different interaction strengths. Depending on its cluster organization, determined by the interaction intensity, the same population thus generated different kinds of collective signals meandering with a number of inward or outward petals. In the final state of full synchronization, the collective signal, however, lost this rich dynamics and became trivially periodic.

Another important aspect of a highly organized multiagent system is its integrity. Interactions between coherent groups span the internal organization. Some groups are brought to existence (i.e., enforced) by the rest of the population. If the activity of a particular group is suppressed, this may entail dramatic changes of the entire organizational structure. These effects were indeed observed in the clustered oscillator populations. Synchronous clusters developed at locations (frequencies) which were different from the maxima in the natural frequency distribution and were thus determined by the interactions among population members. Any two clusters with frequencies ω_1 and ω_2 were responsible for resonant forcing of the entire system at a set of frequencies $n\omega_1 + m\omega_2$, where $n,m =$

§To whom correspondence should be addressed. E-mail: hudson@virginia.edu.

www.pnas.org/cgi/doi/10.1073/pnas.0402899101

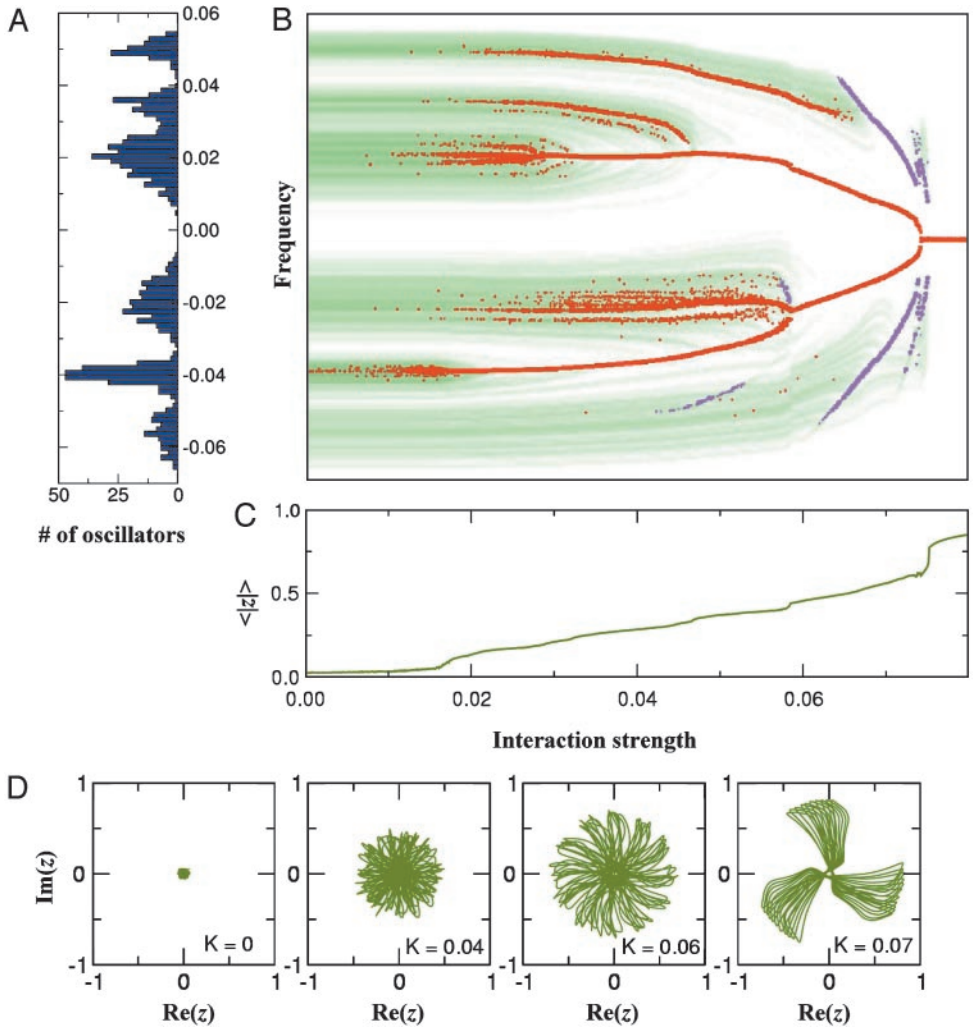

Fig. 1. Simulations for a population of $n = 1{,}000$ interacting phase oscillators. Evolution of phases $\phi_j(t)$ is governed by equations $d\phi_j/dt = \omega_j + (K/N)\Sigma_{k=1}^{N} \sin(\phi_k - \phi_j)$ with $j = 1,2, \ldots, N$, where K is the interaction strength. These equations were numerically integrated by using an Euler scheme with time step $\Delta t = 1$. (*A*) Distribution of natural frequencies, ω_j, in the studied population. (*B*) Distribution of effective frequencies as a function of the interaction strength K. In the color code, darker shades of green indicate the higher local oscillator density. Additionally, clusters are displayed by using red and magenta. A cluster is defined as a group of oscillators whose effective frequencies differ by $<10^{-5}$. Small dots indicate clusters of a size between 5 and 10; large dots correspond to clusters of a size >10. Small clusters of a size <5 are not displayed. Magenta dots indicate resonant clusters. Effective frequencies for each oscillator were computed by averaging $d\phi_j/dt$ over a time interval of 6×10^4 units. (*C*) The average amplitude $\langle |z(t)| \rangle$ of the complex collective signal as a function of the interaction strength. (*D*) Trajectories of $z(t)$ in the complex plane [Re(z), Im(z)] for several values of the interaction strength K, each for a time interval of 3,000. From left to right, $K =$ 0, 0.04, 0.06, and 0.07.

$\pm 1, 2, 3, \ldots$ The forcing shifted the locations of clusters. The population could also respond to such a forcing by forming new coherent groups at some of resonant frequencies. [Resonant clusters have been discussed for external forcing (18).] We identified several resonant clusters in Fig. 1*B*. Note that nonlinear resonant effects were particularly strong when two clusters approached one another, so that their frequencies ω_1 and ω_2 are close. They explain the structural rearrangement that precedes mergers of coherent groups in Fig. 1*B*. The interplay among interacting coherent groups (Fig. 2*A*) can be illustrated through the suppression of the activity of a group of oscillators (Fig. 2*B*) and by applying an external periodic forcing (Fig. 2*C*). Both resulted in a change of the "social" structure of the entire population. Some of the coherent groups completely disappeared, and the frequencies of other, even distant groups underwent substantial change; with forcing several higher-resonance clusters developed.

For a bimodal population, the formation of two synchronized clusters and their subsequent coalescence have been described by Kuramoto (10). Resonant interactions between oscillators have also been considered in the context of neuronal systems and information processing (19, 20). However, the role of resonant interactions in synchronization phenomena and in the restructuring of the oscillator population has not been analyzed so far. Our numerical results show that resonant interactions greatly affect the synchronization process and rich dynamics, including fusion of coherent clusters, can occur.

The aspects of collective behavior considered above in a simple model were investigated in electrochemical experiments. The experimental system was an array of 64 Ni electrodes held at a constant applied potential in sulfuric acid; current, which is proportional to the rate of metal dissolution, was measured on each electrode. The experiments were thus carried out in a well controlled laboratory apparatus appropriate for the study of interacting populations. The inherent local complex dynamics could be controlled by variations in the electrolyte concentration and by applied potential. Heterogeneities occurred both natu-

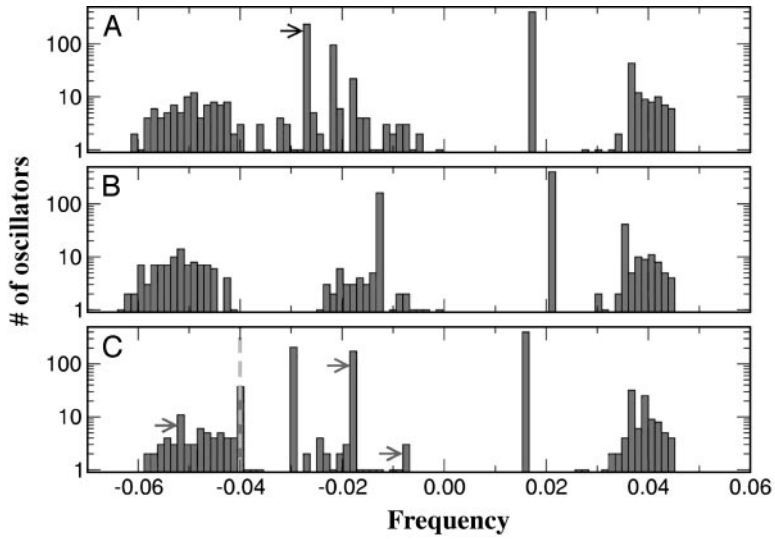

Fig. 2. Responses of the oscillator population to external perturbations. (*A*) Initial distribution of effective frequencies at $K = 0.058$. (*B*) The frequency distribution established when the activity of elements in the cluster marked by the arrow in *A* was suppressed. (*C*) The frequency distribution developed under action of an external force of frequency $\Omega = -0.04$ and intensity $F = 0.001$ (dashed line), applied as an additional term $F\sin(\phi_j - \Omega t)$ to the equations of motion of all oscillators. Several resonant clusters induced by forcing are marked by arrows.

rally through slight differences among the conditions at the metal surfaces and in an enhanced manner via small variations in external resistors. Each electrode or reacting site represents one oscillatory element in the population. Interactions among entities were realized through electrical coupling of individual oscillators.

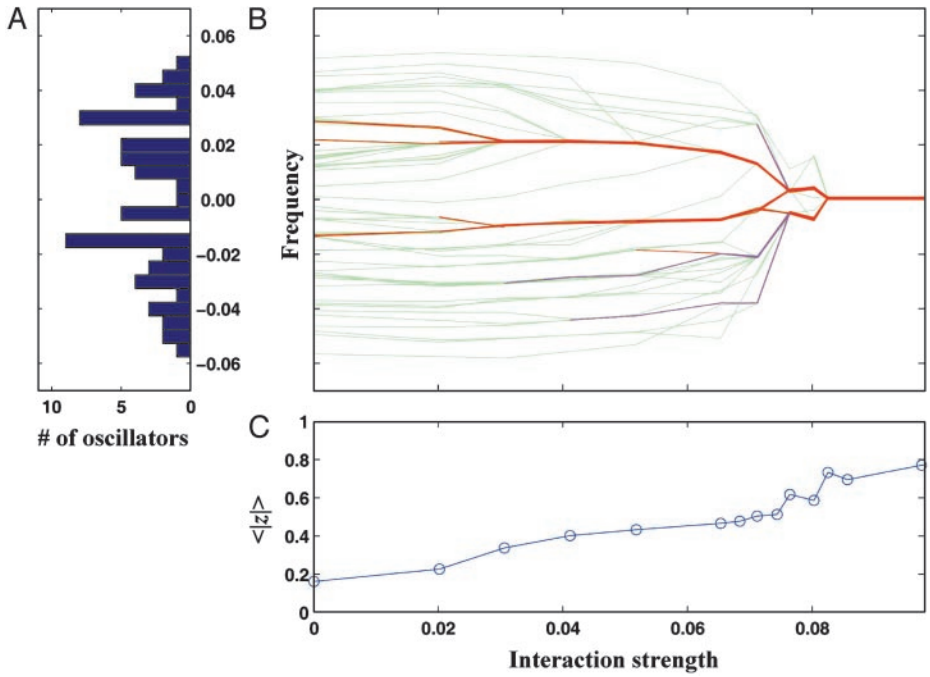

Fig. 3. Experiments on globally coupled 64 nonidentical periodic electrochemical oscillators with multimodal natural frequency distribution. The currents of Ni electrodes (64 1-mm-diameter electrodes in an 8×8 geometry with 2-mm spacing) were measured at 100 Hz. The potential of each electrode was held at constant potential $V = 1.09$ V versus the Hg/Hg_2SO_4/concentrated K_2SO_4 reference electrode. A standard electrochemical cell was used with the Pt mesh counter electrode (see Fig. 5, which is published as supporting information on the PNAS web site; further details can be found in ref. 17). The electrolyte was 3 mol/dm^3 sulfuric acid at 11°C. The electrodes were connected to the potentiostat through one series (collective) resistor, R_s and through 64 parallel resistors, half of which were 100 ohm greater than the rest. The differences in parallel resistors and inherent heterogeneities made the natural frequency distribution have two major peaks. The interaction strength K was controlled through the external resistors $K = (R_s/R_{tot})/(1 - R_s/R_{tot})$, where $R_{tot} = 10.1$ ohm was the total resistance. (*A*) Distribution of dimensionless natural frequencies (at $K = 0$). The dimensionless frequency is defined as $\omega_j = f_j/\langle f\rangle - 1$, where f_j is the frequency of the jth element obtained from a linear fit of phase time series $\phi_j(t)$ and $\langle f\rangle$ is the mean frequency. The phase is the angle in a 2D state space constructed by using the current as the abscissa and its Hilbert transform as the ordinate (21). (*B*) Distribution of dimensionless effective frequencies as a function of the interaction strength K. Thick red and magenta lines show nonresonant and resonant clusters, respectively. (*C*) Dependence of the average magnitude $\langle|z(t)|\rangle$ of the collective signal on K. The collective signal $z(t)$ was calculated from the phases of the oscillating current as in the simulations (for clarity, the mean rotation was eliminated).

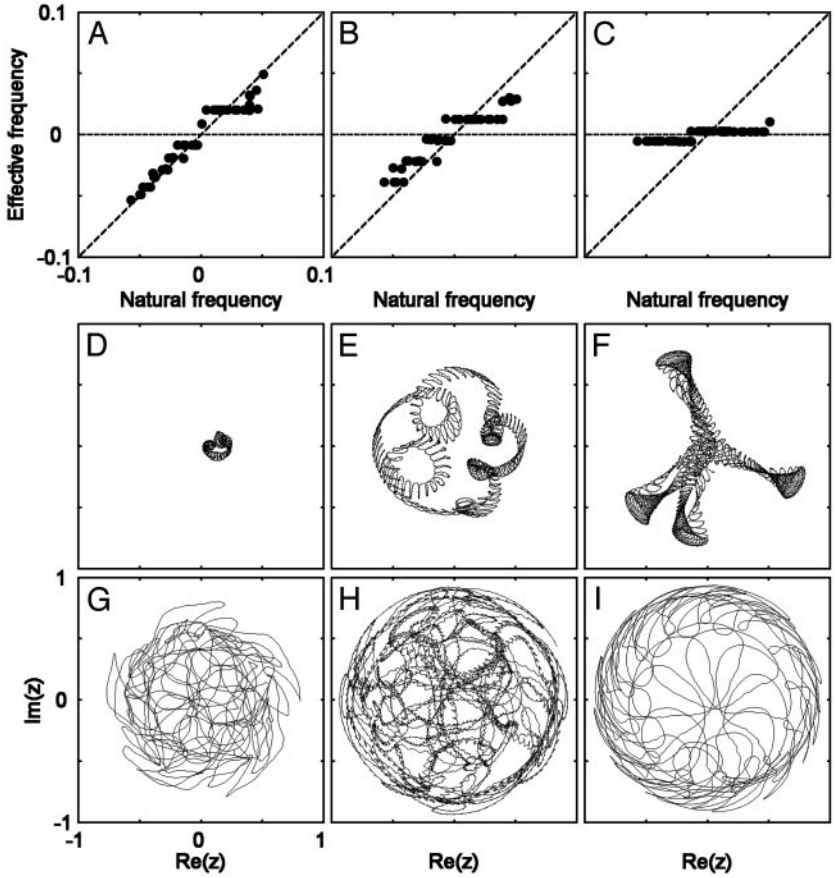

Fig. 4. Experiments on multimodal populations of electrochemical oscillators: the effect of interactions on frequencies and collective signal. (*A–C*) Dimensionless effective frequencies in presence of interactions versus the corresponding natural frequencies in their absence. The uncoupled case ($K = 0$) corresponds to the diagonal line; synchronized clusters yield horizontal line segments. (*D–F*) Trajectories of the collective signal $z(t)$ at different interaction strengths. (*G–I*) Trajectories $z(t)$ at different interaction strengths for another set of experiments where the array was composed of 12 and 52 pieces of wires from two different batches and identical parallel resistors were used ($V = 1.200$ V). As a result, the inherent frequency distribution was less balanced. The interaction strengths K are 0.052 (*A*), 0.071 (*B*), 0.076 (*C*), 0 (*D*), 0.052 (*E*), 0.063 (*F*), 0.052 (*G*), 0.074 (*H*), and 0.109 (*I*).

The effect of interactions is shown in Fig. 3. The natural frequency distribution was approximately bimodal (Fig. 3*A*). The distortion of the frequency distribution by interactions is seen in Fig. 3*B*. Two clusters (groups of elements with the same frequency) at frequencies near the peaks of the natural bimodal distribution emerged at very weak interaction ($K = 0.020$). With increased interactions, the two main groups grew by either incorporating more individual nonentrained elements or by absorbing adjacent smaller clusters. A coherent, synchronized state was observed for $K > 0.083$. The magnitude of the complex signal (Fig. 3*C*) showed the build-up of order with increasing K; larger increases were seen as clusters merged (such as at $K =$ 0.031, 0.076, and 0.083).

The coupling between the two main clusters (having frequencies ω_h and ω_l) and their effects on other elements of the population depended on the strength of interaction. New resonant clusters (magenta) formed at frequencies different from the maxima in the natural frequency distribution; for example, a third ($\omega = \omega_l - \omega_h$), a fourth ($\omega = -2\omega_l - 3\omega_h$), and a fifth ($\omega = 2\omega_h - \omega_l$) cluster arises at $K = 0.031$, 0.042, and 0.071, respectively, as seen in Fig. 3*B*. Effective oscillator frequencies as functions of natural frequencies at three values of K are shown in Fig. 4 *A–C*. A four-cluster state consisting of two main clusters (25 elements at frequency ω_h and 14 at ω_l) and two resonant clusters is seen at $K = 0.052$ (Fig. 4*A*). As in the simulations a major structural rearrangement with strong resonant effects was observed before complete synchronization; at $K = 0.071$ the five clusters have almost equally spaced frequencies with a difference of $\omega_h - \omega_l$ (Fig. 4*B*). Further increase of coupling resulted in a two-clustered state with close frequencies (Fig. 4*C*, $K = 0.076$). The new high- and low-frequency clusters were formed by merging of two high- and two low-frequency groups and by splitting of the remaining (''middle'') cluster (see Fig. 3*B*).

The collective signal $z(t)$, generated by clustered oscillator populations, had rich dynamics (Fig. 4 *D–F*). At $K = 0$, the magnitude of $z(t)$ was small; deviations from zero were due to the finite system size. At $K = 0.052$ and 0.063 it followed a complicated trajectory with inward petal and three-lobe motions, respectively. In Fig. 4 *G–I* the collective signals in the experiments with a different, unbalanced natural frequency distribution are shown (Movies 1–4, which illustrate the collective behavior, are published as supporting information on the PNAS web site).

Despite the significantly higher complexity of the electrochemical reaction system, along with the presence of noise and slow changes of conditions inherent in experiments, the joint action of interacting groups of chemical sites reveals principal properties common with a simple theoretical model of phase oscillators. Spontaneous formation of synchronously operating groups, which endows a population with a capacity to generate complicated collective signals, has been demonstrated. It was found that the emergent structural organization is hierarchical and strongly correlated. Remarkably, some aspects of the ob-

served behavior resemble the features characteristic for much more complex multiagent systems, such as societies or robotic populations. Analogous cooperative action phenomena may also be relevant for the operation of the brain, where properties of neurons on both local and long scales substantially vary and complex collective behavior emerges as the synchronization outcome.

This work was supported by the Humboldt Foundation, Germany (D.H.Z.), and by the National Science Foundation (J.L.H.).

1. Mikhailov, A. S. & Calenbuhr, V. (2002) *From Cells to Societies: Models of Complex Coherent Action* (Springer, Berlin).
2. Manrubia, S. C., Mikhailov, A. S. & Zanette, D. H. (2004) *Emergence of Dynamical Order: Synchronization Phenomena in Complex Systems* (World Scientific, Singapore).
3. Axelrod, R. & Hamilton, W. D. (1981) *Science* **211,** 1390–1396.
4. Bonabeau, E., Dorigo, M. & Theralaulaz, G. (1999) *Swarm Intelligence: From Natural to Artificial Systems* (Oxford Univ. Press, Oxford).
5. Wiener, N. (1958) *Nonlinear Problems in Random Theory* (MIT Press, Cambridge, MA).
6. Winfree, A. T. (1967) *J. Theor. Biol.* **16,** 15–42.
7. Gray, C. M., König, P., Engel, A. K. & Singer, W. (1989) *Nature* **338,** 334–337.
8. Buck, J. (1988) *Q. Rev. Biol.* **63,** 265–289.
9. Walker, T. J. (1969) *Science* **166,** 891–894.
10. Kuramoto, Y. (1984) *Chemical Oscillations, Waves and Turbulence* (Springer, Berlin).
11. Kaneko, K. & Tsuda, I. (2001) *Complex Systems: Chaos and Beyond* (Springer, Berlin).
12. Pecora, L. M. & Carroll, T. L. (1998) *Phys. Rev. Lett.* **80,** 2109–2112.
13. Kiss, I. Z., Zhai, Y. M. & Hudson, J. L. (2002) *Science* **296,** 1676–1678.
14. Golomb, D., Hansel, D., Shraiman, B. & Sompolinsky, H. (1992) *Phys. Rev. A* **45,** 3516–3530.
15. Okuda, K. (1993) *Physica D* **63,** 424–436.
16. Hakim, V. & Rappel, W. J. (1992) *Phys. Rev. A* **46,** R7347–R7350.
17. Wang, W., Kiss, I. Z. & Hudson, J. L. (2000) *Chaos* **10,** 248–256.
18. Sakaguchi, H. (1988) *Prog. Theor. Phys.* **79,** 39–46.
19. Hoppensteadt, F. C. & Izhikevich, E. M. (1998) *Biosystems* **48,** 85–94.
20. Hoppensteadt, F. C. & Izhikevich, E. M. (1999) *Phys. Rev. Lett.* **82,** 2983–2986.
21. Pikovsky, A. S., Rosenblum, M. & Kurths, J. (2001) *Synchronization: A Universal Concept in Nonlinear Science* (Cambridge Univ. Press, Cambridge, U.K.).